Progress In Electromagnetics Research C, Vol. 31, 255–269, 2012

MODIFIED GYSEL POWER DIVIDER WITH HARMONIC SUPPERSSION PERFORMANCE

J. Guan*, L. J. Zhang, Z. Y. Sun, Y. Q. Leng, Y. T. Peng, and Y. P. Yan

Institute of Microelectronics, Chinese Academy of Sciences, No. 3 of Bei-Tu-Cheng West Road, Beijing 100029, China

Abstract—This paper presents a modified Gysel power divider (PD) with harmonic suppression performance by utilizing equivalent Π-shaped, T-shaped and Π-T-hybrid-shaped open stubs transmission line (TL) models. Explicit closed-form expressions for generating parameters of the equivalent TL models are derived based on the *ABCD* matrix analysis. The proposed PD not only features suppression at the hoped harmonic frequencies and flexible layout, but also maintains Gysel PD's high power handling advantage. For demonstration, the simulated and experimental results of three proposed PDs at 1 GHz implemented on microstrip are given.

1. INTRODUCTION

At present, power divider (PD) is widely used in microwave communication and radar systems, such as power splitting/combining networks for microwave power amplifier modules and feeding networks for the antenna arrays. The Wilkinson and Gysel structures are the most popular structures [1–9]. The conventional Wilkinson PD has low insertion loss and high isolation, but its power-handling capability is low. The main advantages of Gysel PD over the Wilkinson PD are (1) its capability of heat transfer to the ground plane because of external isolation load resistors, (2) monitoring capability for imbalances at the output ports [1–8]. Fig. 1 shows the traditional two-way Gysel PD connected with $Z_0 = 50\,\Omega$ character impedance and two load resistors $R_L = 50\,\Omega$ connecting to the ground plane. This traditional Gysel PD is made up of six lines, and the electrical

Received 20 June 2012, Accepted 31 July 2012, Scheduled 3 August 2012

* Corresponding author: Jin Guan (guanjin@ime.ac.cn).

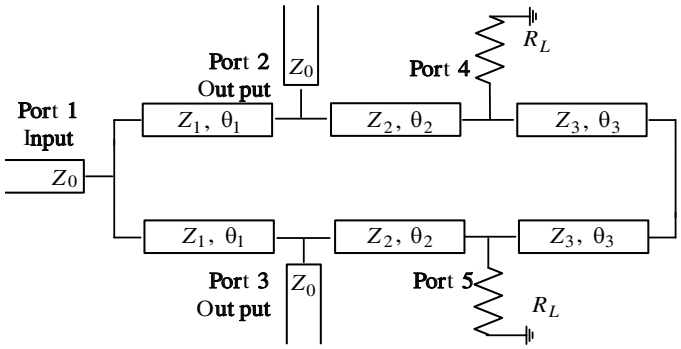

Figure 1. The traditional two-way Gysel PD.

length of each line is 90°. Generally, the impedances of each line are $Z_1 = 70.7\,\Omega$, $Z_2 = 50\,\Omega$, $Z_3 = 35\,\Omega$ (for getting a wider bandwidth, usually choose a lower value of Z_3) [3]. But a major drawback of the conventional PD, hybrids and coupler is the presence of spurious response due to the adoption of quarter-wavelength TL.

Recently, Wilkinson PD, hybrids and coupler with harmonic suppression performance have been studied in some papers. Some studies use defected ground structure (DGS), electromagnetic bandgap (EBG) cells or Non-Uniform Transmission Line to suppress harmonic frequency [10–12] in Wilkinson PD. Though these circuits usually require either backside etching or additional lumped reactive element. Moreover, the design formulas are often not accurate. Papers [13, 14] report Wilkinson PD with harmonic suppression by using shunt stubs with even-odd mode analysis method. Structures without reactive components by using equivalent symmetrical Π-shaped or T-shaped TL model are used to achieve harmonic suppression performance in Wilkinson PD, hybrids and coupler [15–18]. These designs use $ABCD$ matrix TL analysis method, and the equivalent replacement method offers flexible design process and layout.

As far as the authors know, no research of Gysel PD with harmonic suppression performance has been reported. In this paper, unlike the previous papers, we expand to analyze an equivalent replacement method with asymmetric Π-shaped, symmetric T-shaped and asymmetric Π-T-hybrid-shaped TL model to realize one or more harmonic suppression zeros, basing on $ABCD$ matrix analysis. In Section 3, we present a simple process to design the proposed Gysel PD with harmonic suppression characteristic and maintaining high power handling advantage of the original Gysel PD at the fundamental

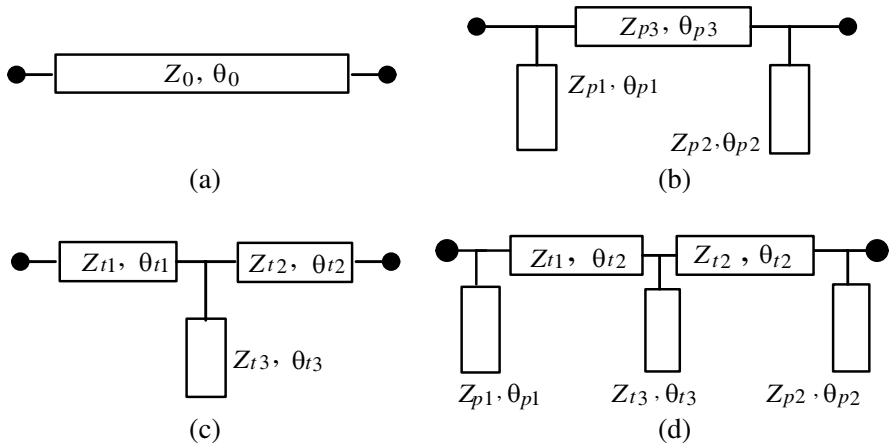

Figure 2. (a) The original TL, (b) the equivalent Π-shaped TL, (c) the equivalent T-shaped TL, (d) the Π-T-hybrid-shaped TL.

frequency. And in Section 4, for illustration, three examples of Gysel PD at a fundamental frequency of 1 GHz are fabricated and tested. This is then followed by conclusion in Section 5.

2. ANALYSIS OF ELEMENT STRUCTURES FOR HARMONIC SUPPRESSION

Figure 2 shows the original TL, equivalent Π-shaped, T-shaped and Π-T-hybrid-shaped TLs. These two equivalent Π-shaped, T-shaped and Π-T-hybrid-shaped TLs can show a similar S-parameter to the original TL at around fundamental frequency. Furthermore, the equivalent TL also shows a bandstop filter character at the specific higher frequencies (in this paper, we just discuss the suppression of harmonic frequencies). In order to achieve the transmission zero at harmonic frequency f_s, which is higher than center frequency f_0, the electrical length θ_s of the open-stub in the equivalent TL modules can be calculated [17] as below

$$\theta_s = \left(\frac{\pi}{2}\right)\left(\frac{f_0}{f_s}\right) \tag{1}$$

General design equations for generating the parameters of the equivalent Π-shaped, T-shaped and Π-T-hybrid-shaped TL are derived by using TL $ABCD$ matrix analysis, as shown below.

2.1. Π-Shaped TL

Shown in Fig. 2(b), the equivalent Π-shaped TL structure which can get two harmonic suppression zeros is comprised of two open-stub lines and one series TL located between the two open-stub. The Z_{pi} is the characteristic impedance (admittance $Y_{pi} = 1/Z_{pi}$) and θ_{pi} the electrical length ($i = 1, 2, 3$). The $ABCD$ matrix of the equivalent Π-shaped TL can be written as (2).

$$M_p = \begin{bmatrix} \cos(\theta_{p3}) - Y_{p2}\tan(\theta_{p2})\sin(\theta_{p3}) & j(Z_{p3}\sin(\theta_{p3})) \\ j(Y_{p1}\tan(\theta_{p1})\cos(\theta_{p3}) + Y_{p3}\sin(\theta_{p3}) - Y_{p1}Y_{p2}Z_{p3}\tan(\theta_{p1})\tan(\theta_{p2}) & -Y_{p1}Z_{p3}\tan(\theta_{p1})\sin(\theta_{p3}) + \cos(\theta_{p3}) \\ \sin(\theta_{p3}) + Y_{p2}\tan(\theta_{p2})\cos(\theta_{p3}) & \end{bmatrix} \tag{2}$$

And the $ABCD$ matrix of the original TL is

$$M_0 = \begin{bmatrix} \cos(\theta_0) & jZ\sin(\theta_0) \\ jY_0\sin(\theta_0) & \cos(\theta_0) \end{bmatrix} \tag{3}$$

To make the original TL equal to the equivalent Π-shaped TL ($M_p = M_0$) at the fundamental frequency, we should make $Y_{p1}\tan(\theta_{p1}) = Y_{p2}\tan(\theta_p 2)$. We will get the results as follow

$$Z_{p1} = \frac{Z_0\sin(\theta_0)\tan(\theta_{p1})}{\cos(\theta_{p3}) - \cos(\theta_0)} \tag{4a}$$

$$Z_{p2} = \frac{Z_0\sin(\theta_0)\tan(\theta_{p2})}{\cos(\theta_{p3}) - \cos(\theta_0)} \tag{4b}$$

$$Z_{p3} = \frac{Z_0\sin(\theta_0)}{\sin(\theta_{p3})} \tag{4c}$$

If we make θ_{p1} and θ_{p2} to be different values to get two suppression zeros, this equivalent Π-shaped TL becomes an asymmetrical TL model. From formulas (4), when we have defined Z_0 and θ_0 (we only discuss $\theta_0 \leq 90^\circ$), the suppression frequencies (getting θ_{p1} and θ_{p2} from formulas (1)) and the limit range of Z_{pi} (microstrip manufacture $25 \sim 135\,\Omega$), we will get the value of Z_{pi} depend on custom variable θ_{p3}.

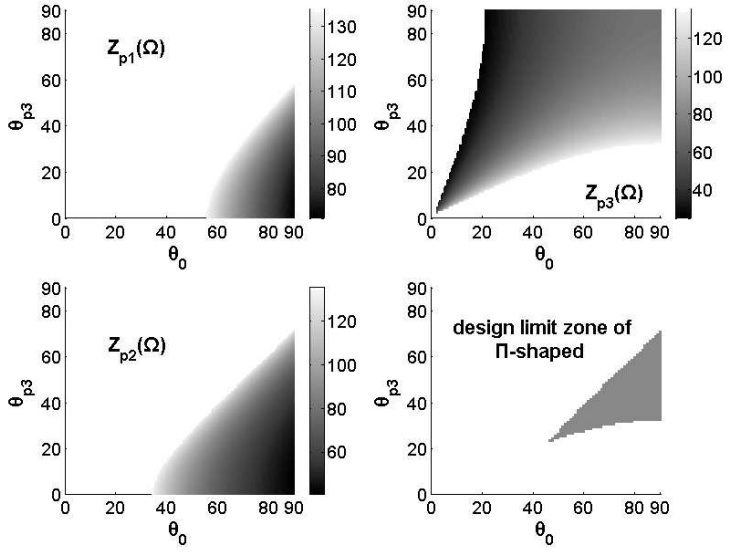

Figure 3. The value of Z_{pi} depend on θ_{p3} vs. θ_0 (when $Z_0 = 70.7\,\Omega$, $\theta_{p1} = 45°$, $\theta_{p2} = 30°$) and the design limit zone of equivalent Π-shaped TL.

Figure 3 shows that the value of Z_{pi} depends on θ_{p3} vs. θ_0, when $Z_0 = 70.7\,\Omega$, $\theta_{p1} = 45°$ and $\theta_{p2} = 30°$. It also shows that the design limit zone of Π-shaped TL depends on θ_{p3} vs. θ_0. This design limit zone of Π-shaped TL can be obtained when the valuable zones of Z_{p1}, Z_{p2} and Z_{p3} are overlapped. When knowing θ_0, we can choose the point in the design limit zone to get the value of θ_{p3}, and then to get the values of Z_{p1}, Z_{p2} and Z_{p3} from Equation (4) or Fig. 3. From Fig. 3, we can see that the higher is Z_{p3}, the lower is $Z_{p1,p2}$ depending on Z_{p3}, so we should choose suitable values to fabricate TL dependent on our own design circuit. Fig. 4 shows that the equivalent Π-shaped TL not only has a similar S-parameter to the original TL at around fundamental frequency, but also has harmonic suppression performance at high frequencies.

2.2. T-Shaped TL

Shown in Fig. 2(c), the equivalent T-shaped TL which can get one harmonic suppression zero is composed of two series TL and one shunt open-stub located between the two series TL. The Z_{ti} is the characteristic impedance (characteristic admittance $Y_{ti} = 1/Z_{ti}$), and θ_{ti} is the electrical length of the TL (i = 1, 2, 3). We use the same

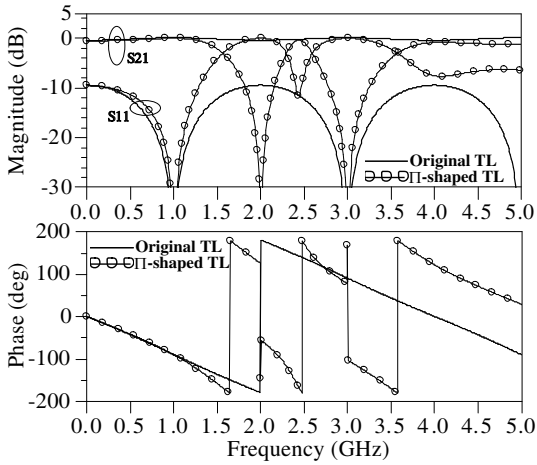

Figure 4. Simulated results (magnitude and phase) of the original TL (70.7 Ω, 90°) and equivalent Π-shaped TL (center frequency = 1 GHz).

method in Section 2.1 to study T-shaped TL. At last, we can get the results as

$$Z_{t1} = Z_{t2} = Z_0 \tan(\theta_0/2) \cot(\theta_{t1}) \tag{5a}$$

$$Z_{t3} = Z_0 \tan(\theta_0/2) \tan(\theta_{t3}) \frac{\cos^2(\theta_{t1})}{\cos(2\theta_{t1}) - \cos(\theta_0)} \tag{5b}$$

Because of making $Z_{t1} = Z_{t2}$ and $\theta_{t1} = \theta_{t2}$, this T-shaped TL becomes a symmetrical model. From formulas (5), when we have defined parameters Z_0 and θ_0 (we only discuss $\theta_0 \leq 90°$), the suppression frequency (getting θ_{t3} from formulas (1)) and the limit range of Z_{ti} (manufacture microstrip $25 \sim 135\,\Omega$), we will get the value of Z_{ti} depending on custom variable θ_{t1}.

Figure 5 shows that the value of Z_{t1} depends on θ_{t1} vs. θ_0, when $Z_0 = 70.7\,\Omega$ and $\theta_{t3} = 30°$. It also shows that the design limit zone of T-shaped TL depends on θ_{t1} vs. θ_0. This design limit zone of T-shaped TL can be obtained when the valuable zones of Z_{t1}, Z_{t2} and Z_{t3} are overlapped. When knowing the θ_0, we can choose the point in the design limit zone to get the value of θ_{t1}, and then to get the values of Z_{t1}, Z_{t2} and Z_{t3} from Equation (5) or Fig. 5. From Fig. 5, we can also see that the higher is $Z_{t1,t2}$, the lower is Z_{t3} depending on θ_{t1}, and we should choose suitable values to fabricate TL depending on our own design circuit. Fig. 6 shows that the equivalent T-shaped TL not only has a similar S-parameter to the original TL at around fundamental frequency, but also has harmonic suppression performance at high frequencies.

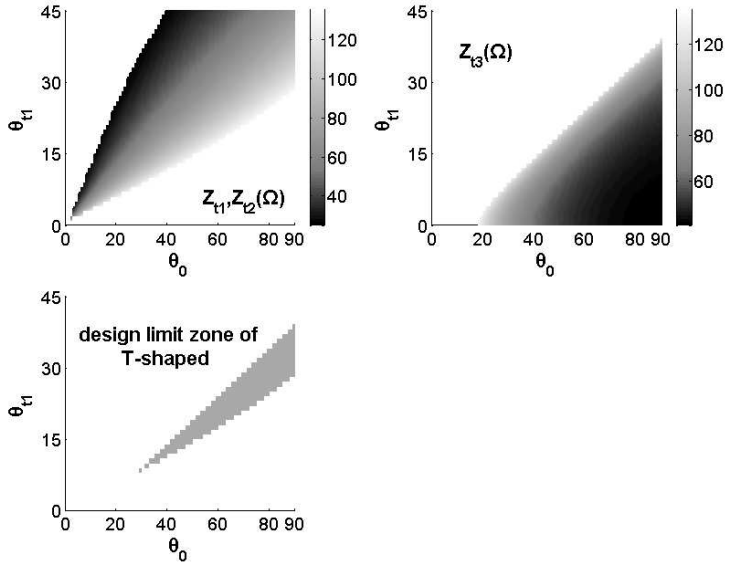

Figure 5. The value of Z_{ti} depend on θ_{t1} vs. θ_0 (when $Z_0 = 70.7\,\Omega$, $\theta_{t3} = 30°$) and the design limit zone of equivalent T-shaped TL.

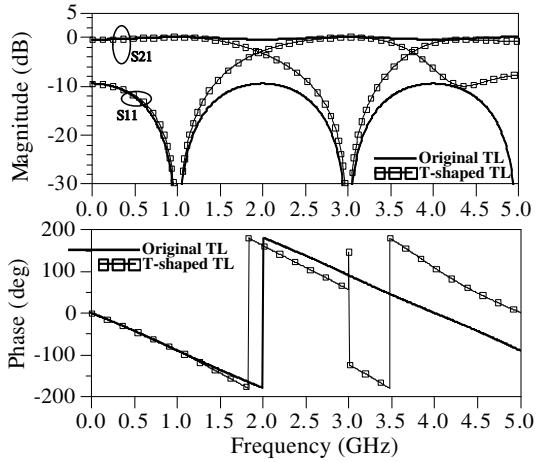

Figure 6. Simulated results (magnitude and phase) of the original TL (70.7 Ω, 90°) and equivalent T-shaped TL (center frequency = 1 GHz).

2.3. Π-T-hybrid-shaped

As shown in Fig. 2(d), we can combine the Π-shaped and T-shaped TLs to get a Π-T-hybrid-shaped TL which can get three harmonic

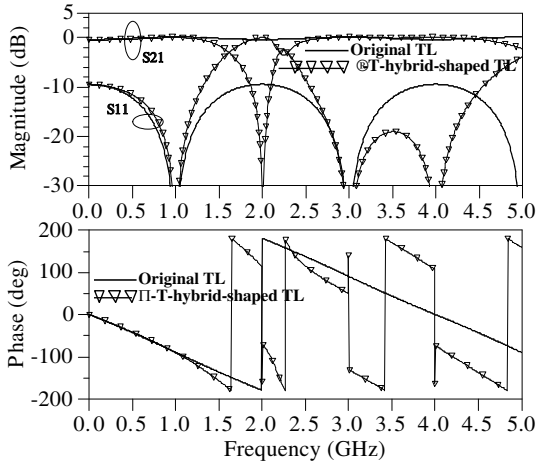

Figure 7. Simulated results (magnitude and phase) of the original TL (70.7 Ω, 90°) and equivalent Π-T-hybrid-shaped TL (center frequency = 1 GHz).

suppression zeros. Firstly, use Π-shaped TL to replace the original TL, and then use the T-shaped TL to replace the TL Z_{p3} located in the middle of Π-shaped TL. The parameters calculations also depend on (4) (5). Fig. 7 shows S-parameter performance of the original and asymmetric Π-T-hybrid- shaped TL.

3. DESIGN PROCEDURE OF PD

By replacing the TL between the input and output ports in the Gysel PD with the equivalent TL module, the modified Gysel PD can provide transmission zeros at higher frequency. As shown in Section 2, this equivalent transmission line replacing method in this paper does not change the S-parameter characters or other characters of TL at the fundamental frequency f_0. So we can deem that the proposed Gysel PD has the same power-handling capability compared with original Gysel PD at the fundamental frequency f_0. Making the design simple, the design procedure of the proposed PD is as follows:

(1) Design a conventional Gysel PD with the parameters of Z_i, θ_i, Z_L and R_L.

(2) Choose the equivalent TL module depending on the required number of the harmonic suppression zeros (T-shape for 1 zero, Π-shape for 2 zeros and T-hybrid-shape for 3 zeros). It means

that the difference among the TLs of the three shapes is that they can achieve different numbers of harmonic suppression zeros, so designers can choose different shape depending on their special circuits design.

(3) Calculate and choose the suitable parameters of the equivalent TL by formulas (1), (4), (5) and Figs. 3, 5, and then use the equivalent TL module to replace Z_1 TL in the Gysel PD.

(4) After the initial design parameters have been obtained, we can simulate, fabricate and test the proposed Gysel PD.

4. SIMULATION AND MEASUREMENT

To verify the proposed structure, three PDs (f_0 = 1 GHz) have been fabricated using microstrip TL on a substrate (Taconic TLX-8) with dielectric constant 2.55, thickness 0.787 mm and loss tangent 0.0021@10 GHz. Table 1 lists the calculated ideal parameter values of three example PDs before any tuning or optimization. The measurement results are collected from an Agilent N5230A network analyzer.

Table 1. Ideal parameter values of three example PDs.

Conventional Gysel PD (Z, R (Ω), θ (deg))		
Z_L, R_L, Z_1, Z_2, Z_3 θ_i (i = 1, 2, 3)		
50, 50, 70.7, 50, 35 90		
1.Π-shaped TL	2.T-shaped TL	3.Π-T-hybrid-shaped TL
Z_{p1}, Z_{p2}, Z_{p3} θ_{p1}, θ_{p2}, θ_{p3}	Z_{t1}, Z_{t2}, Z_{t3} θ_{t1}, θ_{t2}, θ_{t3}	Z_{p1}, Z_{p2}, Z_{p3} θ_{p1}, θ_{p2}, θ_{p3} Z_{t1}, Z_{t2}, Z_{t3} θ_{t1}, θ_{t2}, θ_{t3}
174, 100, 77 45, 30, 66	94, 94, 94 37, 37, 30	174, 100, 77 45, 30, 66 99, 99, 91 27, 27, 22.5

Note: If replacing by two Π-shaped TL in Gysel PD, the two open-stubs Z_{p1} at the input port can be parallel connection to get a lower impendence value, so we can define upper limit of Z_{p1} to 270 Ω.

From Table 1, we can get that two Z_1 TLs with $\theta_0 = 90°$ are substituted by equivalent structures which have a smaller electrical length (θ_{p3} for Π-shaped network, θ_{t1}, θ_{t2} for T-shaped network and θ of series TLs for Π-T-hybrid-shaped network).

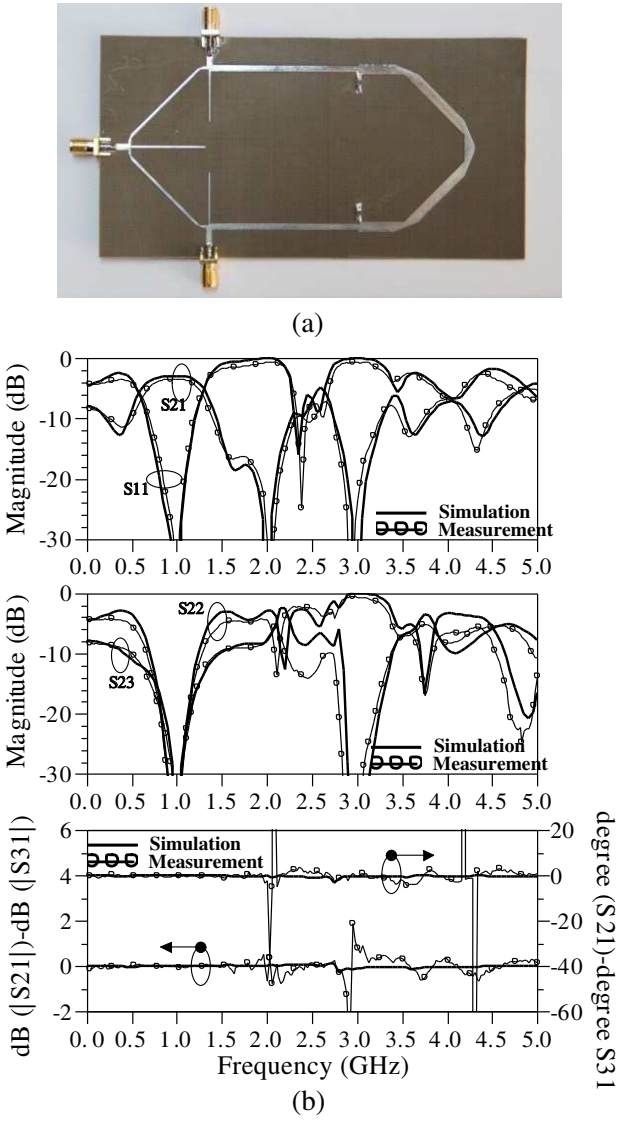

Figure 8. Π-shaped (a) fabricated Gysel PD with equivalent Π-shaped TL. (b) The simulated (EM) and measured S-parameter performance.

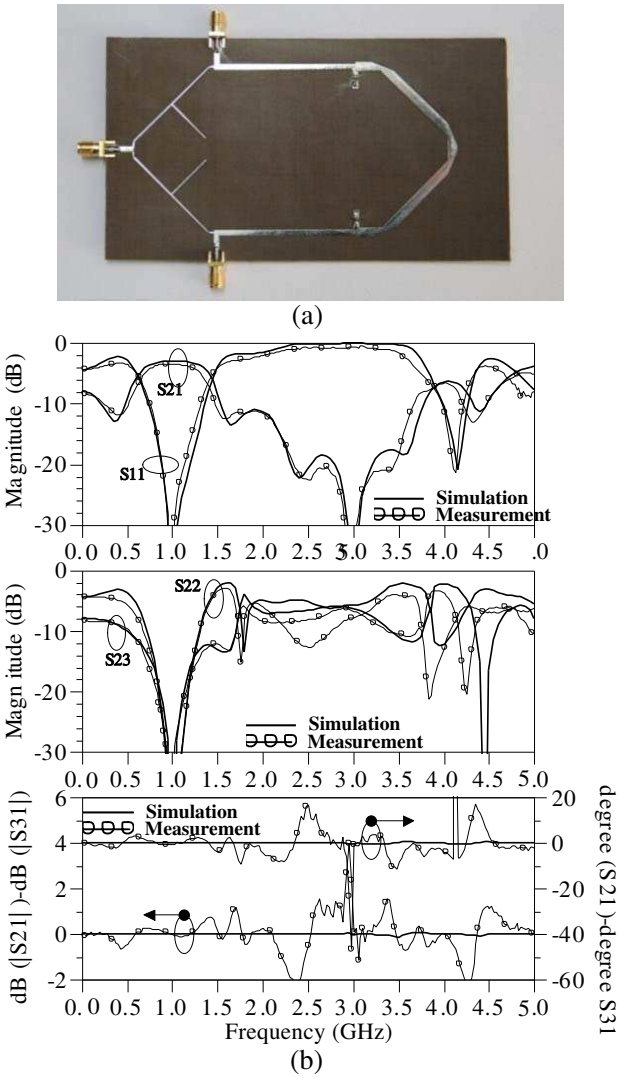

Figure 9. T-shaped (a) fabricated Gysel PD with equivalent T-shaped TL. (b) The simulated (EM) and measured S-parameter performance.

Figures 8–10 show the circuit layouts of the three example PDs with equivalent Π-shaped, T-shaped and Π-T-hybrid-shaped TL and the simulated (EM) and measured S-parameter performances, respectively. The simulated and measured S-parameter performances indicate that Gysel PDs with equivalent TL have been achieved with an attenuation about 30 dB at harmonic frequencies. Inside the fundamental band, the PDs were found to exhibit an insertion loss

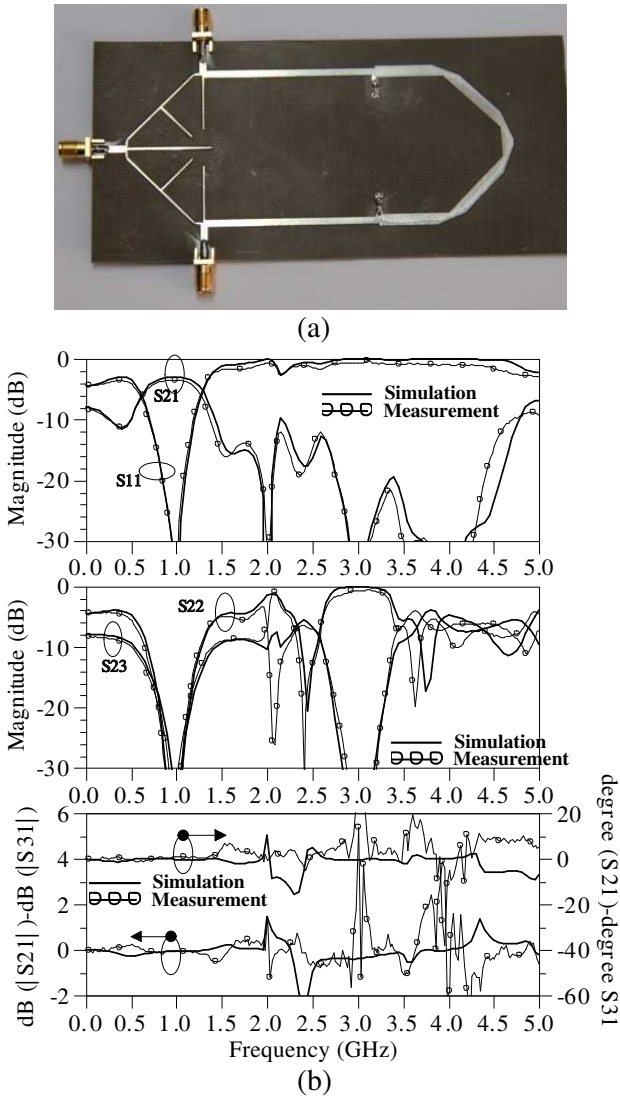

Figure 10. Π-T-hybrid-shaped (a) fabricated Gysel PD with equivalent Π-T-hybrid-shaped TL. (b) The simulated (EM) and measured S-parameter performance.

below about 3.6 dB, minimum input return loss and ports isolation above 30 dB covering a fractional bandwidth of about 30%. And we can also get that at the fundamental frequency, the amplitude imbalance $|S21|$–$|S31|$ and phase imbalance angle($S21$)–angle($S31$) are reasonablly small at the fundamental frequency. We can get

Table 2. Performance (measurement) comparison of three example PDs.

Performance (measurement) comparison of three example PDs			
	1.Π-shaped TL	2.T-shaped TL	3.Π-T-hybrid-shaped TL
Numbers and quantity (dB) of harmonic suppression	Two 27.1 dB @2nd 30.2 dB @3rd	One 34.1 dB@3rd	Three 34.9 dB @2nd 45.6 dB @3rd 38.2 dB @4th
Insertion loss @1 GHz	3.4 dB	3.3 dB	3.4 dB
Return loss @1 GHz	36.3 dB	33.6 dB	33.7 dB
Isolation @1 GHz	38.3 dB	33.4 dB	34.3 dB
Amplitude imbalance $\|\|S21\|-\|S31\|\|$ @1 GHz	<0.1 dB	<0.1 dB	<0.2 dB
Phase imbalance $\|\text{angle}(S21)-\text{angle}(S31)\|$ @1 GHz	$< 1^o$	$< 1^o$	$< 1^o$

Note: Furthermore, the equivalent TL can shows a bandstop filter character at the specific higher frequencies (in this paper, we only discuss the suppression of harmonic frequencies). Design situations are not limited to these three examples.

from Table 2 that the performance (measurement) comparison of three example PDs, which informs the differences among the three proposed Gysel PDs, good suppression at harmonic frequencies and good matching at fundamental frequency.

It is believed that the small discrepancies between the simulated and measured results were mainly caused by the fabrication tolerances, TL losses, discontinuities, SMA connection, and parasitic effect of the surface mounted resistors.

5. CONCLUSION

In this paper, we presents modified Gysel PD with harmonic suppression performance by utilizing equivalent asymmetrical Π-shaped, symmetrical T-shaped and asymmetrical Π-T-hybrid-shaped TL models. The advantages of the proposed Gysel PD with harmonic suppression are that it not only has no any additional lumped elements,

but also has flexible layout and simple design process. Experimental results of the designed PDs agree well with the theoretical predictions. This modified Gysel PD could be applied to microwave circuits and systems which need PDs with not only harmonic suppression performance but also high power handling capability. This simple equivalent replacement design concept should find many applications not only in Gysel PD, but also in other microwave circuits and systems. Additionally, we can see that substituting segments Z_1 with equivalent structures will make a size reduction. We deduce that if we substitute segments Z_1, Z_2, Z_3 in the same time, the size will become even smaller. We will research this character in our future paper.

ACKNOWLEDGMENT

This work was supported in part by the National Basic Research Program of China (973 Program, No. 2010CB327506).

REFERENCES

1. Gysel, U. H., "A new N-way power divider/combiner suitable for high-power applications," *IEEE-MTT-S International Microwave Symposium*, 116–118, 1975.
2. Wilkinson, E. J., "An N-way hybrid power divider," *IRE Transactions on Microwave Theory and Techniques*, Vol. 8, 116–118, 1960.
3. Ardemagni, F., "An optimized L-band eight-way gysel power divider-combiner," *IEEE Transactions on Microwave Theory and Techniques*, Vol. 31, 491–495, 1983.
4. Fartookzadeh, M., S. H. Mohseni Armaki, and M. Kazerooni, "A novel 180° hybrid based on the modified gysel power divider," *Progress In Electromagnetics Research C*, Vol. 27, 209–222, 2012.
5. Zhang, H., X.-W. Shi, F. Wei, and L. Xu, "Compact wideband gysel power divider with arbitrary power division based on patch type structure," *Progress In Electromagnetics Research*, Vol. 119, 395–406, 2011.
6. Wu, Y., Y. Liu, and S. Li, "An unequal dual-frequency Wilkinson power divider with optional isolation structure," *Progress In Electromagnetics Research*, Vol. 91, 393–411, 2009.
7. Deng, P.-H., J.-H. Guo, and W.-C. Kuo, "New Wilkinson power dividers based on compact stepped-impedance transmission lines and shunt open stubs," *Progress In Electromagnetics Research*, Vol. 123, 407–426, 2012.

8. Li, B., X. Wu, N. Yang, and W. Wu, "Dual-band equal/unequal Wilkinson power dividers based on coupled-line section with short-circuited stub," *Progress In Electromagnetics Research*, Vol. 111, 163–178, 2011.
9. Sun, Z. Y., L. J. Zhang, Y. P. Yan, and H. W. Yang, "Design of unequal dual-band gysel power divider with arbitrary termination resistance," *IEEE Transactions on Microwave Theory and Techniques*, Vol. 59, 1955–1962, 2011.
10. Shamaileh, K. A. A., A. M. Qaroot, and N. I. Dib, "Non-uniform transmission line transformers and their application in the design of compact multi-band Bagley power dividers with harmonics suppression," *Progress In Electromagnetics Research*, Vol. 113, 269–284, 2011.
11. Duk-Jae, W. and L. Taek-Kyung, "Suppression of harmonics in Wilkinson power divider using dual-band rejection by asymmetric DGS," *IEEE Transactions on Microwave Theory and Techniques*, Vol. 53, 2139–2144, 2005.
12. Lin, C. M., H. H. Su, J. C. Chiu, and Y. H. Wang, "Wilkinson power divider using microstrip EBG cells for the suppression of harmonics," *IEEE Microwave and Wireless Components Letters*, Vol. 17, 700–702, 2007.
13. Yi, K.-H. and B. Kang, "Modified Wilkinson power divider for nth harmonic suppression," *IEEE Microwave and Wireless Components Letters*, Vol. 13, 178–180, 2003.
14. Cheng, K. K. M. and W.-C. IP, "A novel power divider design with enhanced spurious suppression and simple structure," *IEEE Transactions on Microwave Theory and Techniques*, Vol. 58, 3903–3908, 2010.
15. Mondal, P. and A. Chakrabarty, "Design of miniaturised branch-line and rat-race hybrid couplers with harmonics suppression," *IET Microwaves, Antennas & Propagation*, Vol. 3, 109–116, 2009.
16. Mondal, P. and A. Chakrabarty, "Harmonic suppression and size reduction of planar rat- race hybrid couplers," *Asia-Pacific Microwave Conference, APMC*, 671–673, 2006.
17. Srisathit, K., P. Jadpum, and W. Surakampontorn, "Miniature Wilkinson divider and hybrid, coupler with harmonic suppression, using T-shaped transmission line," *Asia-Pacific Microwave Conference, APMC*, 1–4, 2007.
18. Velidi, V. K. and A. Bhattacharya, "A stub tapped compact hybrid coupler with broad-band harmonic rejection," *TENCON 2008 — IEEE Region 10 Conference*, 1–5, 2008.